

# Chemical, mineralogical, and environmental characterisation of stibnite and its alteration products (San Antonio Mine, Badajoz)

Joana Gabriela Paim Figueira (1), Ascensión Murciego (1\*), Esther Álvarez-Ayuso (2), Jesús Medina (3), Aurelio Sanz Arranz (3), Fernando Rull (3)

(1) Department of Geology. University of Salamanca, Plaza de los Caídos, s/n, 37008 Salamanca (Spain)

(2) Department of Environmental Geochemistry. IRNASA (CSIC), C/Cordel de Merinas, 40-52, 37008 Salamanca (Spain)

(3) Unidad Asociada UVa-CSIC-Centro de Astrobiología, C/ Francisco Valles 8, Boecillo (Spain)

\* corresponding author: [murciego@usal.es](mailto:murciego@usal.es)

**Palabras Clave:** Estibina, Cervantita, Grupo roméita, Lixiviación. **Key Words:** Stibnite, Cervantite, Roméite group, Leaching.

## INTRODUCTION

The oxidation of sulphides present in wastes of abandoned mining areas is a process that can generate contamination by the release of metals/metalloids (e.g., antimony) and acid mine drainage. In the San Antonio mine (Badajoz), where the most important antimony deposit in Europe was exploited, there are dumps containing stibnite ( $\text{Sb}_2\text{S}_3$ ). The aim of this work is the chemical-mineralogical characterisation of this mineral and its oxidation products and the evaluation of the potential environmental risk of these mine dumps.

## MATERIALS AND METHODS

The studied samples consist of fragments of bedrock and quartz veins with partially altered stibnite (Fig. 1a). The alteration products appear as earthy crusts, yellow, orange, or brownish in colour, forming a protective layer over stibnite. Their mineralogical and chemical characterisation was carried out by X-ray diffraction (XRD), polarized light microscopy in transmitted and reflected light, electron microprobe, and micro-Raman spectroscopy. The environmental characterisation was conducted out on 3 types of samples: a) stibnite, b) stibnite and its alteration products, and c) stibnite alteration products. The following processes and determinations were carried out: leaching test, bioavailability test, chemical fractionation, pH and net neutralisation potential.

## RESULTS AND DISCUSSION

The minerals identified by XRD are quartz, muscovite, stibnite, cervantite ( $\text{Sb}^{3+}\text{Sb}^{5+}\text{O}_4$ ) and roméite-group minerals ( $\text{A}_2\text{B}_2\text{X}_6\text{Y}$  formula:  $\text{Sb}^{5+}$  predominates in the B-site;  $\text{Ca}^{2+}$ ,  $\text{Pb}^{2+}$ ,  $\text{Fe}^{2+}$ ,  $\text{Na}^{2+}$ ,  $\text{Sb}^{3+}$ , and others in the A-Site and  $\text{OH}^-$ ,  $\text{O}^{2-}$ ,  $\text{F}^-$  in the Y-Site, determining different minerals in the group). Gumiel & Arribas (1987) cited stibiconite ( $\text{Sb}^{3+}\text{Sb}^{5+}_2\text{O}_6(\text{OH})$ ), cervantite, and goethite ( $\alpha\text{-FeOOH}$ ) as the main supergene minerals in this mine. The microscopic study in reflected light showed that stibnite is the major sulphide. It occurs in both unaltered and fully altered crystals, and in relics with corroded edges within the alteration products constituted by three phases exhibiting different shades of grey (Fig. 1b). In transmitted light microscopy the mineral closest to stibnite is colourless and yellowish with high interference colours. It is a scarce mineral in the studied samples, and it could correspond to native sulphur, generated by the incongruent dissolution of stibnite (Biver & Shotyk, 2012). Native sulfur is bordered by a mineral with yellowish and brownish tones and anisotropic, identified as cervantite, closely linked and replaced by a colourless and brownish mineral with a cloudy appearance and isotropic, belonging to the roméite-group (Fig. 1c). Thus, the alteration sequence is stibnite-sulphur-cervantite-roméite group minerals. The chemical analysis (expressed in wt. %) revealed that stibnite is quite pure (Sb: 71.07-71.57, S: 27.86-28.49); only the  $\text{SnO}_2$  content (0.12-0.21) is noteworthy. Cervantite analyses show  $\text{Sb}_2\text{O}_5$  contents between 96.13 and 98.69 and the presence of  $\text{SO}_3$  (0.08-3.54),  $\text{SnO}_2$  (0.15-0.27),  $\text{FeO}$  (<l.d.-0.51),  $\text{As}_2\text{O}_5$  (<l.d.-0.12),  $\text{WO}_3$  (<0.08), and  $\text{MnO}$ ,  $\text{NiO}$ , and  $\text{CoO}$  (<0.04). Roméite shows  $\text{Sb}_2\text{O}_5$  and  $\text{CaO}$  contents in the ranges of 75.28-81.23 and 3.47-7.25, respectively, and low contents of other elements such as  $\text{FeO}$  (0.03-1.03),  $\text{SnO}_2$  (0.09-0.23),  $\text{Na}_2\text{O}$  (0.09-0.33),  $\text{SO}_3$  (0.01-2.17),  $\text{As}_2\text{O}_5$  (<d.l.-0.07),  $\text{CoO}$  (<d.l.-0.03),  $\text{TiO}_2$  (<d.l.-0.14), and  $\text{MnO}$  (<d.l.-0.04). The low total contents of roméite

analyses may be due to the porous nature of the samples and the presence of vacancies and/or water molecules. The abundance of vacancies at the A site is not ruled out because of the low Ca contents in the roméite of this work, compared to other roméites (Lopes et al., 2021). This would indicate a low availability of Ca in the medium. Additionally, the  $\text{Sb}_2\text{O}_5$  contents are higher than those of other roméites; this could be due to the existence of  $\text{Sb}^{3+}$  at the A position. The microRaman spectra of stibnite and cervantite show similar bands to those observed by Makreski et al. (2013) and the spectra of roméite exhibit a characteristic band at around  $520\text{ cm}^{-1}$  but no band corresponding to  $\text{H}_2\text{O}$  is observed. Native sulfur, not analysed, was identified by its microRaman spectrum.

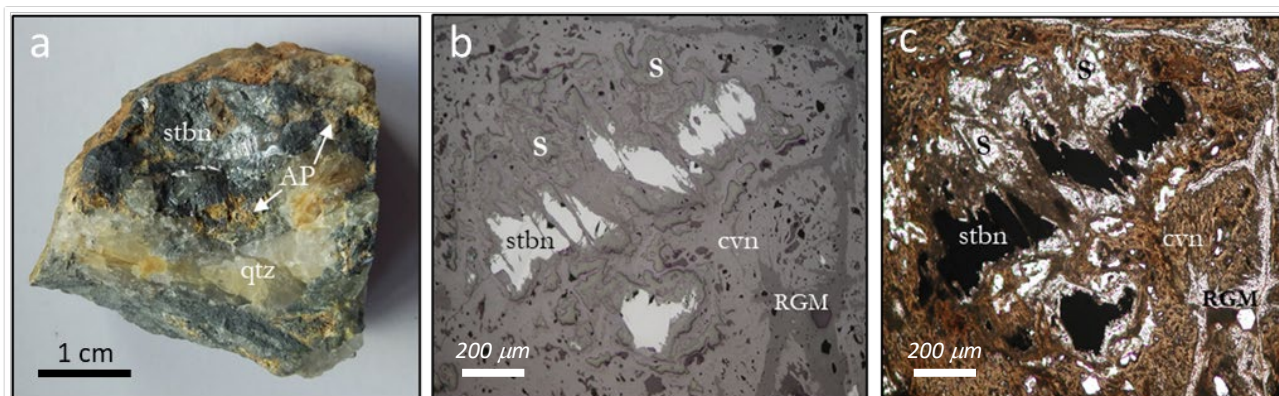


**Fig 1.** Hand sample (a) and reflected (b) and transmitted light (c) microscopy images. *Stbn*: stibnite, *qtz*: quartz, *AP*: alteration products, *cvn*: cervantite, *S*: native sulfur, *RGM*: roméite-group minerals.

The leachable Sb contents (mg/kg) in the three types of samples (stibnite: 1113, altered stibnite: 676, and stibnite alteration products: 1604) exceed very widely the limit value (5 mg/kg) for the acceptance of wastes at hazardous waste landfills. Likewise, the bioavailable Sb contents (mg/kg) are very high in the different samples studied (stibnite: 1069, altered stibnite: 437, and alteration products: 605). Conversely, the bioavailable As is very low ( $< 1.5\text{ mg/kg}$ ) in all these samples, whereas Mo has a relatively high bioavailable content in the altered stibnite sample (17.1 mg/kg). The Sb distribution in the stibnite and altered stibnite samples shows the following sequence: residual  $\gg$  oxidisable  $>$  reducible  $>$  acid soluble, while for the alteration products the sequence is: residual  $\gg$  oxidisable  $>$  acid soluble  $>$  reducible. In all cases, Sb is distributed mostly in the residual fraction (97.2-98.6 %). The distribution of Sb in the oxidisable fraction shows relatively low values (1-2 %), while in the acid soluble and reducible fractions is  $< 1\%$ . The acid soluble fraction of stibnite and altered stibnite shows the lowest Sb values (around 0.1 %) and that of the alteration products the highest (0.90 %). Therefore, the Sb mobilisation that would occur under changes in environmental conditions such as acidification or establishment of reducing conditions is relatively restricted with respect to the total Sb contents. However, it would entail a significant environmental risk since in absolute terms it involves the release of high levels of Sb. The aqueous extracts of the altered stibnite samples and the alteration products have an acid pH, whereas that of the stibnite sample is very close to neutral values. Only the altered stibnite sample is clearly acid generating, showing a net neutralisation potential of  $-160\text{ kg CaCO}_3/\text{t}$  which is much lower than the value below which materials are considered acid generating ( $-30\text{ kg CaCO}_3/\text{t}$ ).

## ACKNOWLEDGMENTS

The present study was carried out under the project TERMET (Grant number: RTI2018-095433-B-I00) funded by Ministerio de Ciencia, Innovación y Universidades (MCIU), Spain/Agencia Estatal de Investigación (AEI), Spain/Fondo Europeo de Desarrollo Regional (FEDER), UE.

## REFERENCES

- Biver, M. & Shotyk, W. (2012): Stibnite ( $\text{Sb}_2\text{S}_3$ ) oxidative dissolution kinetics from pH 1 to 11. *Geochim. Cosmochim. Acta*, **79**, 127-139.
- Gumiel, P. & Arribas, A. (1987): Antimony deposits in the Iberian Peninsula. *Econ. Geol.*, **82**, 1453-1463.
- Makreski, P., Petrusevski, G., Ugarkovic, S., Jovanovski, G. (2013): Laser-induced transformation of stibnite ( $\text{Sb}_2\text{S}_3$ ) and other structurally related salts. *Vib. Spectrosc.*, **68**, 177-182.
- Lopes, G.A.C., Atencio, D., Ellena, J., Andrade, M.B. (2021): Roméite-Group Minerals Review: New Crystal Chemical and Raman Data of Fluorcalciroméite and Hydroxycalciroméite. *Minerals*, **11**, 1409.